GEOCHEMICAL PHASE DIAGRAMS AND GALE DIAGRAMS

P.H. EDELMAN, S.W. PETERSON, V. REINER, AND J.H. STOUT

Abstract. The problem of predicting the possible topologies of a geochemical phase diagram, based on the chemical formula of the phases involved, is shown to be intimately connected with and aided by well-studied notions in discrete geometry: Gale diagrams, triangulations, secondary fans, and oriented matroids.

Contents

1991 *Mathematics Subject Classification.* 52B35, 52C40, 86A99.

Key words and phrases. Gale diagram, Gale transform, phase diagram, triangulation, secondary polytope, secondary fan, geochemistry, heterogeneous equilibrium, closed net, Euler sphere.

Work of second author was carried out partly as a Masters Thesis at the University of Minnesota Center for Industrial Mathematics, and partly supported by a University of Minnesota Grant-in-Aid of Research. Third author was partially supported by NSF grant DMS–9877047.

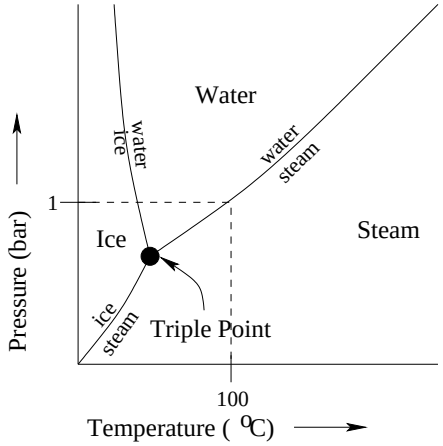

FIGURE 1. The phase diagram for the simple chemical system with phases ice, water, and steam.

1. INTRODUCTION

A central problem in geochemistry has been to understand how the equilibrium state of a chemical system varies with temperature and pressure, and predict the form of its temperature-pressure phase diagram (hereafter called just the *phase diagram*). The purpose of this paper is to explain how some recently developed tools from discrete geometry (the theory of oriented matroids, triangulations, Gale diagrams, and secondary fans) can be used to elucidate this problem. Our goal is to be comprehensible to both discrete geometers and workers in geochemistry.

Figure 1 illustrates the familiar phase diagram for a simple chemical system that involves three phases (ice, water, steam) of the same chemical compound, H_2O. The topological structure of this diagram is fairly simple: there is a unique point, called a triple point, where all three phases can be present in equilibrium. The triple point lies at the junction of three curves. Along each of these curves exactly two of the phases are present in equilibrium (either ice + water, or ice + steam, or water + steam), and these three curves separate two-dimensional

regions where only one phase (pure ice, or pure water, or pure steam) can be present in equilibrium.

This example of a phase diagram is quite an elementary one, in that all the phases have the same underlying chemistry, that of H_2O. Geochemists are interested in phase diagrams as the principal tool in reconstructing the temperature and pressure conditions from rock formations once deep within the Earth but which now reside at its surface. Thus it is important to have accurate phase diagrams involving much more complex systems in which the phases have different chemistry as well as different states.

To be more precise, a *phase* means a physically homogeneous substance, having its own chemical formula, although different phases within the system can have the same formula (as in the ice-water-steam example). At a particular temperature and pressure, the equilibrium state consists of groups of one or more phases that are referred to as *phase assemblages*. Within a closed system at fixed temperature and pressure, only certain phase assemblages will be stable, namely those having the lowest possible *Gibbs free energy* under the given conditions. Other assemblages with higher energy than the minimum under those conditions are referred to as *metastable* – these assemblages react spontaneously to produce a stable assemblage and a net decrease in energy. For example, pure water placed in the stability field of ice will spontaneously freeze because a lower Gibbs energy assemblage (ice) is available under those conditions. When there are different chemical formulae present among the phases, more exotic reactions than simple phase changes are possible. The regions of simultaneous stability for various collections of phase assemblages, and the chemical reactions that relate them are conveniently summarized in the phase diagram.

The locus of temperatures and pressures within which a particular phase assemblage is stable is called its *stability field*. The stability field is called *invariant*, *univariant*, or *divariant* depending upon its dimension, that is, the number of degrees of freedom one can vary while staying within that stability field. In the example above, the triple point (ice-water-steam) is an invariant point, there are three univariant curves (ice-water, ice-steam, water-steam), and three divariant stability fields (pure ice, pure water, pure steam). The univariant fields correspond to simple chemical reactions that transform one phase assemblage to another, and hence are sometimes referred to as *reaction lines*. In producing these phase diagrams, a prediction of the possible topologies (i.e. number of invariant points, number of univariant curves joining them, etc.) is indispensable, as the thermodynamic data

needed to resolve such topological features can sometimes be difficult to obtain.

It turns out that much of the complexity of the phase diagram for a chemical system is governed by two parameters:

- the number of phases, m, and
- the number of components, n (defined below).

We will see in Section 3 that these two parameters correspond to the *size of the ground set* and the *rank* of a related vector configuration (or affine point configuration, or oriented matroid) associated with the chemical system. It is well-known, in both geochemistry and discrete geometry, that what matters most in predicting the complexity of the phase diagram is not the sizes of n and m, but rather the sizes of n and $m-n$ (the rank and the *co-rank*).

The *number of components* n for a chemical system is defined as follows. Think of the chemical formulae of the various phases of the system as vectors in a vector space of all possible such formulae (the *chemical composition space*– see Section 3), whose coordinate axes correspond to the elements present on Earth. Then the number n of components of the chemical system is simply the dimension of the subspace spanned by the chemical formulae of the phases present in the system[1]. For example, the system of ice, water and steam from Figure 1 has $m = 3$ phases and $n = 1$, while the system depicted in Figure 2 has $m = 4$ phases and $n = 2$.

Phase diagram topologies for chemical systems with $m \leq n + 2$ are fairly well-understood, even as m grows large. For $m \leq n + 1$ they are essentially trivial, and for $m = n + 2$, they look roughly like Figure 1, having an invariant point surrounded by several univariant reaction curves. The schematic picture of such an invariant point surrounded by reaction curves is referred to as an *invariant point map* [17]. We will explain in Section 8 why invariant point maps look roughly like a *two-dimensional Gale diagram*, in concordance with rules for the phase diagram's construction first delineated by Schreinemakers [25] nearly 100 years ago.

However, by $m = n + 3$ (a situation common for chemical systems applicable to the Earth) the topology of the phase diagram can become quite complex as m grows large. For example, under certain genericity assumptions about the chemical formulae of the phases, the diagram

[1]It will be convenient in Section 3 to choose a basis for this space, that is a minimal set of phases such that all the formulae of the phases can be expressed as linear combinations of these basic components; hence the term *number of components* of the system.

will contain exactly $n+3$ invariant points located at various temperature and pressure coordinates. These invariant points are connected to one another by various reaction lines to a form a network of points and lines referred to by geochemists as a *petrogenetic grid*. For example, a typical grid for $n = 4$ and $m = 7$ will have 7 invariant points connected by 21 different reaction lines.

The phase diagram topology of this (as well as higher order systems) has been represented schematically by geochemists via a *straight line net*, made up of a set of invariant point maps linked together by common reaction lines. In Section 9 we will explain how straight line nets for systems with $m = n + 3$ can be constructed using *3-dimensional Gale diagrams* and *secondary fans*, and hence why their phase diagrams strongly resemble the encoding of a 3-dimensional Gale diagram as a 2-dimensional *affine Gale diagram*.

Within the geochemical literature, there are two general approaches to reconstructing the topology of the phase diagram. The first approach was pioneered by Schreinemakers [25] who reasoned about relative Gibbs energies of phases to deduce invariant point maps for $m = n+2$. This method has been extended by various authors ([29], [31], [32]; [6]; [16], and references therein) to produce viable straight line nets for systems with $m = n+3$. All feasible topologies are enumerated by this method and then empirical data is used to eliminate those diagrams which are physically impossible. This approach can be made much more efficient by the methods described in this paper.

The alternative approach is to compute the variation in Gibbs energy directly for every phase of interest. Modern thermodynamic databases (e.g., [13] and references therein) now make these computations possible. The method fails in some cases because the data either lacks the accuracy to distinguish between topologically different diagrams or is simply not available for some phases. The latter situation is becoming more common as new phases are discovered by laboratory synthesis under high pressure conditions. The quantities of these phases are so small that the necessary thermodynamic data will not be available in the foreseeable future. Thus geochemists must rely on the topological approach developed earlier.

We should point out that there have been a few authors [12, 27] who have given a somewhat similar mathematical formulation of this problem, but without taking advantage of the language, techniques and highly developed theory provided by Gale diagrams and oriented matroids. The applications derived in Section 10 of this paper are, as far as we know, new. Furthermore, the theory described in this paper is the basis for JAVA applets written by the second author and available

on the web [18], which give practical tools for use in geochemistry to predict phase diagram topology.

2. A geochemistry-discrete geometry dictionary

For the convenience of the reader, and as a guide to what lies in store, we present a (very rough) dictionary of corresponding terms.

Geochemistry	Discrete geometry
chemical formula for a phase	vector in composition space
chemical system	acyclic vector configuration $\mathcal{V}$
chemography	affine point configuration $\mathcal{A}$
number of phases m	number of vectors/points
number of components n	rank of vector/point configuration
reactions among phases	linear/affine dependences of $\mathcal{V}/\mathcal{A}$
minimal reactions	circuits
stable assemblage of phases	simplex in a triangulation of $\mathcal{A}$
phase diagram	affine plane slice of secondary fan
phase diagram when $m = n + 2$	2−dimensional Gale diagram $\mathcal{A}^*$
reaction half-line for $m = n + 2$	vector in 2−dim'l Gale diagram $\mathcal{A}^*$
phase diagram when $m = n + 3$	2−dim'l affine Gale diagram for $\mathcal{A}^*$
invariant point when $m = n + 3$	vector in 3−dim'l Gale diagram $\mathcal{A}^*$
closed net when $m = n + 3$	spherical representation of $\mathcal{A}^*$
Euler sphere for $m = n + 3$	great circles normal to $\mathcal{A}^*$

3. Chemical composition space

In this section, we introduce the chemical composition space that allows one to associate to each chemical system a configuration of vectors, an affine point configuration, and their oriented matroid. For terminology on vector configurations, point configurations and oriented matroids, we refer the reader to two excellent references: the bible of the subject [2] (in particular, its §1.2), and Ziegler's book [33, Lecture 6].

Definition 3.1. The formulae of chemical compounds may be represented in a natural way by vectors in a *chemical composition space* whose axes are indexed by the elements in the periodic table. For example, H_2O has coordinates which are two units on the hydrogen axis, one unit on the oxygen axis, and zero on all other axes. The m phases of a chemical system in this way give rise to a collection $\mathcal{V} = \{v_1, \ldots, v_m\}$ of vectors spanning a subspace of some dimension n, which is called the *number of components* of the system. By picking a basis for this

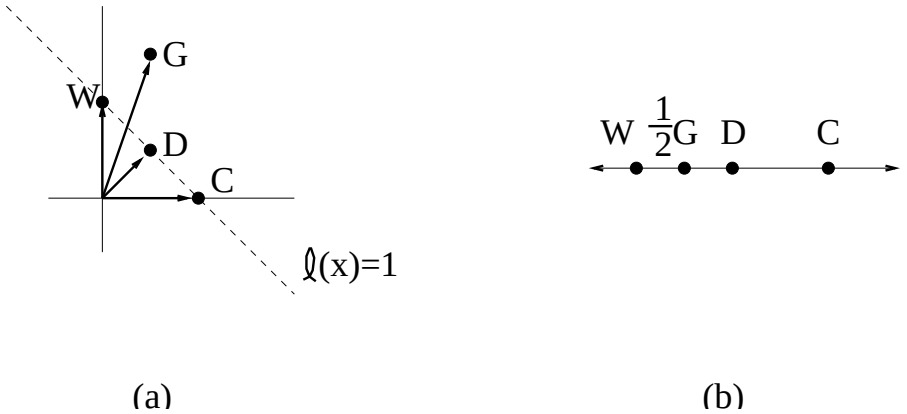

FIGURE 2. (a) Vector configuration $\mathcal{V}$, and (b) affine point configuration $\mathcal{A}$ for the chemical system with phases corundum (C), diaspore (D), gibbsite (G), and water (W).

subspace, we can identify it with $\mathbb{R}^n$ and specify each v_i by a column vector in $\mathbb{R}^n$. This allows us to identify $\mathcal{V}$ with an $n \times m$ matrix having full rank n, which we also call $\mathcal{V}$ by an abuse of notation.

Example 3.2. Consider a chemical system of relevance to geology having $m = 4$ phases, which we denote by descriptive initials rather than v_1, v_2, v_3, v_4:

$$\begin{array}{lll} C = & \text{corundum} & Al_2O_3 \\ D = & \text{diaspore} & AlO(OH) \\ G = & \text{gibbsite} & Al(OH)_3 \\ W = & \text{water} & H_2O. \end{array} \tag{1}$$

Since the compounds in this system involve only the elements Al, O, H, this system can have n at most 3. But one can check that these chemical formulae span a space of dimension $n = 2$. Choosing C and W to be the standard basis vectors in this space (that is, the *components* for this system), one can represent the configuration $\mathcal{V}$ as the columns of

the following matrix

$$\mathcal{V} = \begin{array}{c} \begin{matrix} C & D & G & W \end{matrix} \\ \begin{bmatrix} 1 & \frac{1}{2} & \frac{1}{2} & 0 \\ 0 & \frac{1}{2} & \frac{3}{2} & 1 \end{bmatrix} \end{array} \tag{2}$$

and the associated vector configuration is depicted in Figure 2(a).

Notice that by choosing a basis that identifies this n-dimensional subspace with $\mathbb{R}^n$, we are already abstracting away from the actual chemical formulae of the phases and paying attention only to properties that are invariant under a simultaneous change-of-basis acting on the vectors, that is, properties invariant under $GL_n(\mathbb{R})$. One such set of properties is the oriented matroid associated to the vector configuration $\mathcal{V}$.

Definition 3.3. The *oriented matroid* $\mathcal{M}$ associated to $\mathcal{V}$ is a combinatorial abstraction of the vectors $\mathcal{V}$ which forgets their actual coordinates, but retains data specifying the signs involved in linear dependences among the v_i. The way in which we choose to record this data is to list the *signed circuits* of $\mathcal{M}$ coming from each minimal (non-trivial) linear dependence $\sum_i \lambda_i v_i = 0$, that is, the *signed set* (X^+, X^-) where

$$X^{\pm} := \{i \in \{1, \ldots, m\} : \mathrm{sign}(\lambda_i) = \pm\}.$$

Here minimality for signed sets is interpreted with respect to the ordering of their *support sets*:

$$(X^+, X^-) < (Y^+, Y^-) \text{ means } X^+ \cup X^- \subseteq Y^+ \cup Y^-.$$

It is sometimes convenient to represent a signed set (X^+, X^-) instead by its *sign vector* in $\{+, 0, -\}^m$ which has $\pm$ in the coordinates indexed by $X^{\pm}$, and 0 in all other coordinates. For example, a minimal dependence of the form $+5v_1 - 3v_2 + \frac{7}{8}v_4$ among $m = 4$ phases would be recorded by the circuit whose signed set is $(\{1, 4\}, \{2\})$ or by its sign vector $(+ - 0+)$.

It is possible to write down a small set of *circuit axioms* satisfied by by the set $\mathcal{C}$ of signed circuits coming from any vector configuration, in such a way that collections of signed sets satisfying these axioms (*oriented matroids*) mimic many features of sets of vectors in a real vector space– see [2, p. 4]. Note that since the negation of a linear dependence gives another linear dependence, one of these circuit axioms for an oriented matroid says that the set of sign vectors of circuits is closed under negation.

The linear dependences among the v_i have an obvious chemical intepretation: they are the coefficients in the mass-preserving chemical reactions possible among the phases.

Example 3.4. Continuing the previous example, there are three minimal linear dependences/reactions, giving rise to the following signed circuits (represented by two opposite sign vectors below):

minimal reaction/dependence	circuits as sign vectors
$G \rightleftharpoons 1D + 1W$	$0+-+, \quad 0-+-$
$2D \rightleftharpoons 1C + 1W$	$+-0+, \quad -+0-$
$3D \rightleftharpoons 1C + 1G$	$+-+0, \quad -+-0$

Note that another possible reaction among these phases is

$$1C + 2W \rightleftharpoons 1D + 1G$$

which would give rise to dependences with sign vectors

$$+--+, \quad -++-$$

but these are not signed circuits because their support sets are not minimal under inclusion.

The fact that every chemical compound contains a non-negative amount of each element implies that the vector configuration $\mathcal{V}$ will be *acyclic*, that is, there will be no signed circuits with $X^- = \{\varnothing\}$. Equivalently, there exists a linear functional $\ell(x)$ in $(\mathbb{R}^n)^*$ such that $\ell(v_i) > 0$ for all i. This allows one to replace each v_i by a rescaled vector a_i satisfying $\ell(a_i) = 1$, so that the a_i lie in the affine hyperplane $\ell(x) = 1$ inside $\mathbb{R}^n$, giving rise to an *affine point configuration*[2] $\mathcal{A}$ in $(n-1)$-dimensional affine space $\mathbb{R}^{n-1}$. In chemical terms, this replacement corresponds to simply changing conventions for writing down basic quantities of each phase: instead of considering one mole to be the basic unit of quantity for some phase, one can consider a half a mole or some other fraction to be its basic unit of quantity[3].

The effect of this rescaling is to turn linear dependences $\sum_i \lambda_i v_i = 0$ of the original vector configuration $\mathcal{V}$ into *affine dependences* of $\mathcal{A}$, that is, relations $\sum_i \bar{\lambda}_i a_i = 0$ with $\sum_i \bar{\lambda}_i = 0$. In terms of chemical reactions,

[2]In [17], this affine point configuration $\mathcal{A}$ is called the *chemography* of the system.

[3]We have already pointed out that two phases can have the same chemical formula, giving rise to two copies of the same vector $v_i = v_j$ in $\mathcal{V}$; these give rise to what are called *parallel elements* of the oriented matroid $\mathcal{M}$. We should note however that parallel elements can also arise after doing the rescaling from $\mathcal{V}$ to $\mathcal{A}$ if two phases have chemical formula which differ by a scalar multiple, e.g. if both oxygen O_2 and ozone O_3 were present as phases.

this means that the reactions will not only achieve mass-balance for each atom, but also "coefficient balance", as in the following example.

Example 3.5. Continuing the previous example, we can choose the linear function $\ell(x) = x_1 + x_2$ in $\mathbb{R}^2$ and rescale the coordinates of C, D, G, W so that they have $\ell(x) = 1$, giving the new matrix

$$\mathcal{A} = \begin{array}{c} \begin{matrix} C & D & \frac{1}{2}G & W \end{matrix} \\ \begin{bmatrix} 1 & \frac{1}{2} & \frac{1}{4} & 0 \\ 0 & \frac{1}{2} & \frac{3}{4} & 1 \end{bmatrix} \end{array} \tag{3}$$

The affine point configuration in $\mathbb{R}^1$ represented by $\mathcal{A}$ is depicted in Figure 2 (b).

The rescaling in this case only required replacing G by $\frac{1}{2}G$, so that, for example the previous reaction/linear dependence

$$1G \rightleftharpoons 1D + 1W$$
$$1Al(OH)_3 \rightleftharpoons 1AlO(OH) + 1H_2O$$

which achieves mass-balance for each atom but not coefficient balance ($1 \neq 1 + 1$), now gives rise to the affine dependence

$$2 \cdot \left(\frac{1}{2}G\right) \rightleftharpoons 1D + 1W,$$

achieving coefficient balance: $2 = 1 + 1$.

Switching from the vector configuration $\mathcal{V}$ to the affine point configuration has psychological advantages, in that it allows one to reduce the dimension by one for visualization purposes, and it makes it easier to think about our next topic: triangulations[4] of $\mathcal{A}$.

4. Triangulations and subdivisions

Our goal in this section is to explain a phenomenon well-known to geochemists: by performing reactions that minimize the Gibbs free energy resulting in a stable phase assemblage at a particular temperature and pressure, Nature (generically) "computes" a triangulation of the point set $\mathcal{A}$.

Having fixed a temperature and pressure (T, P), each of the phases $a_1, \ldots, a_m$ of the chemical system will have a certain *Gibbs free energy*

[4]We should point out that there is a well-defined notion of triangulations for general vector configurations (even when they are not acyclically oriented), as well as for oriented matroids that do not come from configurations of vectors. See [24] and the references contained therein.

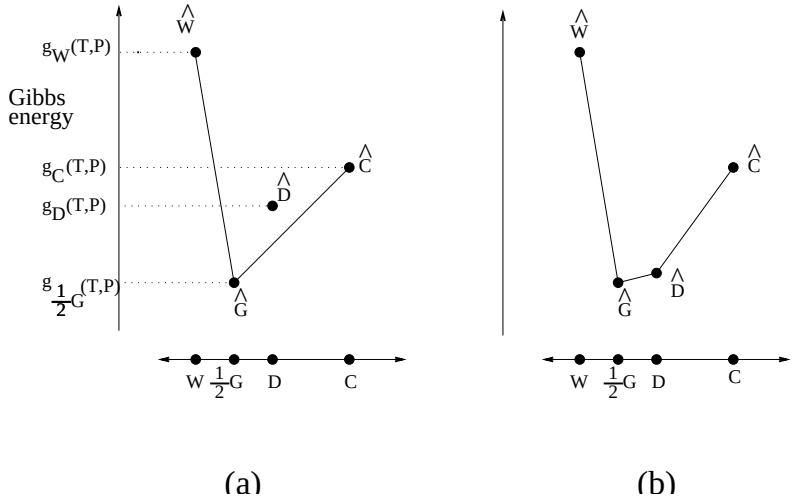

FIGURE 3. The chemography $\mathcal{A}$ from Figure 2, "lifted" to $\hat{\mathcal{A}}$ by the Gibbs energy values at two different values of temperature and pressure.

$g_i(T, P)$ per molar quantity (or per whatever basic quantity is being used after rescaling v_i to a_i).

Definition 4.1. These values $g_i(T, P)$ can be used as *heights* to "lift" the points a_i in $\mathbb{R}^{n-1}$ to points

$$\hat{a}_i := \begin{bmatrix} a_i \\ g_i(T,P) \end{bmatrix} \quad \in \mathbb{R}^n,$$

giving a new *lifted* configuration of points $\hat{\mathcal{A}}$. In other words, we plot the points a_i together with their height along an extra *Gibbs energy axis*; see Figure 3 for two examples having $n = 2$.

The *convex hull*, that is the set of all convex combinations, of this set $\hat{\mathcal{A}}$ of lifted points has the following physical interpretation. Suppose we have an assemblage consisting of x_i units of the basic quantity of phase a_i for each $i = 1, \ldots, m$, and assume (without loss of generality) that $\sum_i x_i = 1$. Then this assemblage will have total Gibbs energy $\sum_i x_i g_i(T, P)$, which is the same as the height on the Gibbs energy axis

of the point $\sum_i x_i \hat{a}_i$ which is a weighted average of the lifted points $\hat{\mathcal{A}}$, and therefore lies somewhere in their convex hull. If this point does not lie on the *lower convex hull* of these lifted points, then this is not a stable assemblage of phases: there exist some reaction(s) available which would alter the fractions of each phase a_i in a way that lowers the total Gibbs energy.

Example 4.2. We continue our previous example, and assume that the Gibbs energies of the phases are as depicted in Figure 3(a). Consider the assemblage consisting of $\frac{1}{2}$ mole of C together with $\frac{1}{2}$ mole of D. It lifts to the point $\frac{1}{2}\hat{C} + \frac{1}{2}\hat{D}$ at the midpoint of the line segment $\hat{C}\hat{D}$ in Figure 3(a), whose height $\frac{1}{2}g_C(T_0, P_0) + \frac{1}{2}g_D(T_0, P_0)$ represents the total Gibbs energy of this assemblage. It is not stable because one can run the reaction

$$3D \leftrightharpoons 1C + 1G$$

in the forward direction to convert the $\frac{1}{2}$ mole of D into $\frac{1}{6}$ mole each of C and G. This creates an assemblage with lower total Gibbs energy consisting of $\frac{2}{3}$ mole of C together with $\frac{1}{6}$ mole of G (or equivalently, $\frac{1}{3}$ mole of $\frac{1}{2}G$). The latter assemblage however is stable, as it lifts to a point on the segment $\hat{C}\hat{G}$ lying in the lower convex hull of $\hat{\mathcal{A}}$.

On the other hand, if the Gibbs energies of the phases looked as they do in Figure 3(b), then the initial assemblage of $\frac{1}{2}$ mole of C together with $\frac{1}{2}$ mole of D would have been stable, and no reactions would occur.

Note that even after the temperature and pressure (T, P) have been fixed, there can be more than one possible stable assemblage, and which stable assemblages appear depends upon the initial quantities of each phase present. In petrology, when one takes various samples from different locations inside a stratum of rock formed under the same temperature and pressure conditions, one has a chance of sampling from all the different stable assemblages.

From the previous discussion, we conclude that the sets of phases which can form stable assemblages correspond to the sets of vertices which lie on a face of the lower convex hull of $\hat{\mathcal{A}}$. Note that projecting these faces of the lower hull in $\mathbb{R}^n$ down into $\mathbb{R}^{n-1}$ produces a set of convex polytopes that disjointly cover the convex hull of $\mathcal{A}$, forming what is usually called a *polytopal subdivision* of $\mathcal{A}$. If the vector

$$g = (g_1(T, P), \ldots, g_m(T, P)) \in \mathbb{R}^m$$

is sufficiently generic, then each of the faces of the lower convex hull will be an $(n-1)$-dimensional *simplex* (that is, the convex hull of n

affinely independent points), and this polytopal subdivision is called a *triangulation* of $\mathcal{A}$; see [10, Chapter 7] for formal definitions.

Definition 4.3. Triangulations and polytopal subdivisions of $\mathcal{A}$ which are induced in this fashion from a vector of heights $g = (g_1, \ldots, g_m)$ in $\mathbb{R}^m$ are called *coherent* or *regular*, and we call $\Delta(g)$ the subdivision induced by g.

We summarize here some of the conclusions of the preceding discussion.

Proposition 4.4. *For each fixed temperature and pressure (T, P), the vector*

$$g = g(T, P) := (g_1(T, P), \ldots, g_m(T, P)) \in \mathbb{R}^m$$

of Gibbs energies for the phases $\mathcal{A} = \{a_1, \ldots, a_m\}$ induces a coherent polytopal subdivision $\Delta(g)$ of $\mathcal{A}$.

The polytopes participating in this subdivision have vertex sets corresponding exactly to the stable assemblages of phases at that temperature and pressure (T, P).

It is perhaps surprising that in general not all triangulations of a point configuration $\mathcal{A}$ need be coherent. In Figure 4 we show an affine configuration with 6 points in $\mathbb{R}^2$ with two incoherent triangulations. This example is well-known in the discrete geometry literature (see e.g. [10, Chapter 7, Figure 27]), and is the "smallest" example due to the following result.

Theorem 4.5. [15] *When either $n \leq 2$ or $m - n \leq 2$, every triangulation of an affine point configuration of m points in $\mathbb{R}^{n-1}$ is coherent.*

Bearing Proposition 4.4 in mind, in order to understand the topology of the phase diagram for a chemical system, one needs to understand how the coherent subdivision $\Delta(g)$ of a point configuration $\mathcal{A}$ varies with the height vector g in $\mathbb{R}^m$. This is our next goal.

5. Secondary fans

The goal of this section is to introduce the secondary fan $\mathcal{F}(\mathcal{A})$, and its close relative, the pointed secondary fan $\mathcal{F}'(\mathcal{A})$, which govern how the coherent subdivisions $\Delta(g)$ of $\mathcal{A}$ change as one varies the height vector g in $\mathbb{R}^m$. Some references for this material are [3, §4], [10, Chapter 7].

Having fixed a particular affine point configuration $\mathcal{A}$ of m points in $\mathbb{R}^{n-1}$, one can ask when two height vectors g and g' in $\mathbb{R}^m$ give rise to the same subdivision Δ. It should come as no surprise that the set of vectors g which give rise to a particular subdivision Δ forms a polyhedral cone $\mathcal{C}(\mathcal{A}, \Delta) \subset \mathbb{R}^m$, that is, it is defined by a finite set of

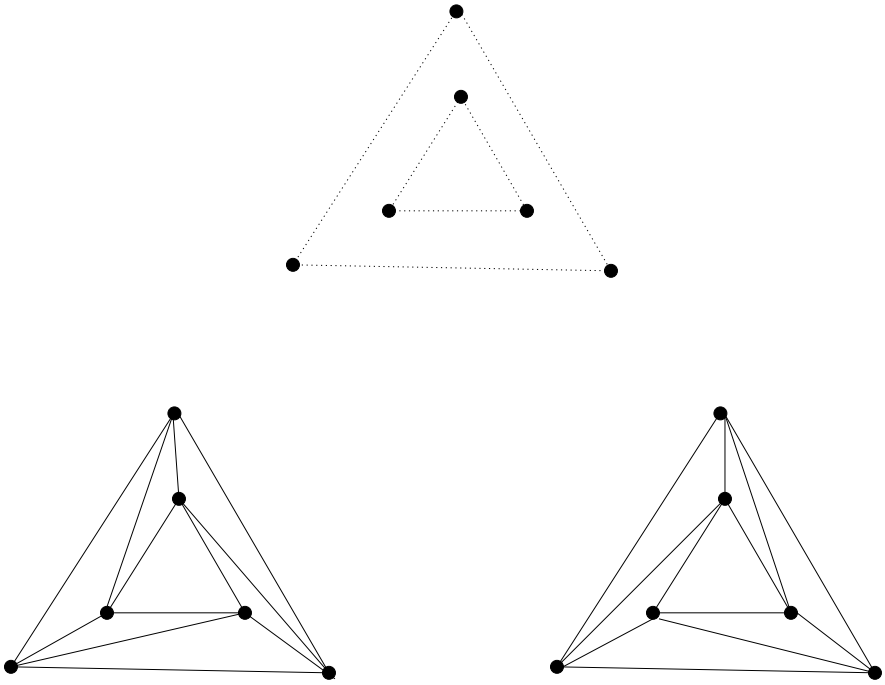

FIGURE 4. Incoherent triangulations of an affine point configuration $\mathcal{A}$: the standard, smallest example, along with its two incoherent triangulations.

linear inequalities (which depend on the coordinates of the points $\mathcal{A}$ and on Δ). As one varies the subdivision Δ, these cones $\mathcal{C}(\mathcal{A}, \Delta)$ fit together to disjointly cover $\mathbb{R}^m$.

Definition 5.1. In the terminology of discrete geometry, these cones form a *(complete) fan* called the *secondary fan* $\mathcal{F}(\mathcal{A})$; see Figure 5(a) for the example of ice-water-steam from the Introduction[5].

[5]Although we are not aware of a geochemical intepretation, we should point out a beautiful result of Gelfand, Kapranov, and Zelevinsky asserting that the secondary fan $\mathcal{F}(\mathcal{A})$ is actually the *normal fan* of a convex polytope, which they called the *secondary polytope* $\Sigma(\mathcal{A})$; see [10, Chapter 7]. One should also be aware of a slight difference in focus when referring to their results, which they mainly prove for $\Sigma(\mathcal{A})$, but which can then be translated into results about $\mathcal{F}(\mathcal{A})$.

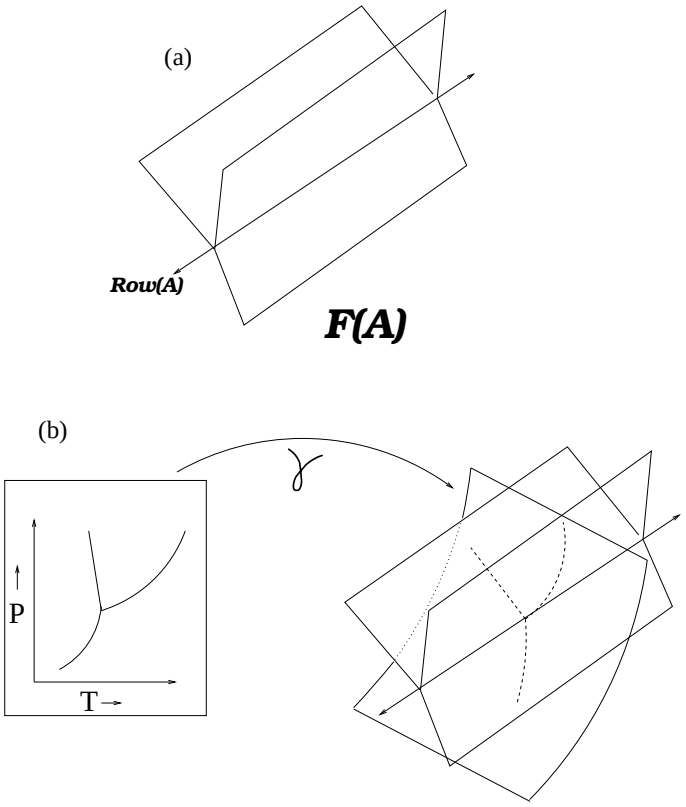

FIGURE 5. For the chemical system of ice, water, and steam with $n = 1$ and $m = 3$, we have (a) the secondary fan $\mathcal{F}(\mathcal{A})$, (b) The image surface $\gamma(\mathbb{R}^2)$ decomposed by $\mathcal{F}(\mathcal{A})$, and the phase diagram as the pull-back of this decomposition.

We can now rephrase precisely what the phase diagram means in these terms.

Definition 5.2. Consider the (T, P)-plane in which the phase diagram is drawn as a copy of $\mathbb{R}^2$. Then the Gibbs energy functions $g_i(T, P)$ for the m phases can be viewed as specifying a *Gibbs energy map*

$$\begin{array}{rccl} \gamma: & \mathbb{R}^2 & \to & \mathbb{R}^m \\ & (T,P) & \mapsto & g(T,P) \ = (g_1(T,P),\ldots,g_m(T,P)). \end{array}$$

The image $\gamma(\mathbb{R}^2)$ of this map will be some 2-dimensional surface in $\mathbb{R}^m$. The decomposition of $\mathbb{R}^m$ into the cones of the secondary fan $\mathcal{F}(\mathcal{A})$ will restrict to a decomposition of this surface $\gamma(\mathbb{R}^2)$; see Figure 5(b) for the example of ice-water-steam. This decomposition of the surface then *pulls back* to induce a decomposition of the (T, P)-plane $\mathbb{R}^2$ into regions, which are the regions of simultaneous stability for various collections of phase assemblages (i.e. two pairs $(T, P), (T', P')$ lie in the same region of the phase diagram if and only if their images under γ lie in the same cone of $\mathcal{F}(\mathcal{A})$). In other words, we have the following statement, illustrated in Figure 5(b):

Proposition 5.3. *The phase diagram for a chemical system having chemography $\mathcal{A}$ is exactly the decomposition of the (T, P)-plane $\mathbb{R}^2$ which is the pull-back under γ^{-1} of the decomposition of the image surface $\gamma(\mathbb{R}^2)$ induced by the cones of the secondary fan $\mathcal{F}(\mathcal{A})$.*

Thus understanding possible phase diagram topologies amounts to understanding the structure of the secondary fan $\mathcal{F}(\mathcal{A})$ and the Gibbs energy map γ well enough to predict how the fan $\mathcal{F}(\mathcal{A})$ can decompose 2-dimensional surfaces $\gamma(\mathbb{R}^2)$ in $\mathbb{R}^m$.

It turns out that there is a natural way to cut down the dimension of $\mathcal{F}(\mathcal{A})$ by the number of components n, without losing any information. Recall that $\mathcal{A}$ also denotes the $n \times m$ matrix whose columns are the n-vectors a_i (with each of these column vectors lying in the affine hyperplane $\ell(x) = 1$). It is not hard to see that two height vectors g and g' which differ by a vector lying in the row space $\mathrm{Row}(\mathcal{A})$ of this matrix $\mathcal{A}$ will induce the same coherent subdivision Δ: one can show that the two configurations of lifted points they produce will differ by an affine transformation of $\mathbb{R}^n$, and consequently their convex hulls will differ only by a "tilt" that does not affect the structure of their lower hulls. As a consequence, each of the cones $\mathcal{C}(\mathcal{A}, \Delta)$ in the secondary fan $\mathcal{F}(\mathcal{A})$ extends trivially in the n directions defined by $\mathrm{Row}(\mathcal{A})$; it is a Cartesian product

$$\mathcal{C}(\mathcal{A}, \Delta) = \mathcal{C}'(\mathcal{A}, \Delta) \times \mathrm{Row}(\mathcal{A})$$

where $\mathcal{C}'(\mathcal{A}, \Delta)$ is a cone in an $(m - n)$-dimensional subspace of $\mathbb{R}^m$ complementary[6] to $\mathrm{Row}(\mathcal{A})$. As Δ varies over all coherent subdivisions, these cones $\mathcal{C}'(\mathcal{A}, \Delta)$ disjointly cover this complementary $(m-n)$-dimensional subspace, producing what is called the *pointed secondary fan* $\mathcal{F}'(\mathcal{A})$.

[6]It would be more natural to think of the cones $\mathcal{C}'(\mathcal{A}, \Delta)$ as living in the *quotient space* $\mathbb{R}^m/\mathrm{Row}(\mathcal{A})$, but we won't quibble here

We next make explicit the simplifying assumption which is implicit in the geochemical literature on this subject.

Geochemical assumption 5.4. *Over the ranges of temperature and pressure $(T, P) \in \mathbb{R}^2$ relevant to most phase diagrams, the Gibbs energy map $\gamma : \mathbb{R}^2 \to \mathbb{R}^m$ is sufficiently close to linear that the image surface $\gamma(\mathbb{R}^2)$ behaves nearly like a 2-dimensional affine plane in $\mathbb{R}^m$.*

Furthermore, this 2-dimensional affine plane is located generically with respect to the cones of the secondary fan $\mathcal{F}(\mathcal{A})$ in the following sense: it has transverse intersection with every cone $\mathcal{C}$ in the secondary fan (including the smallest face which is the row space $\mathrm{Row}(\mathcal{A})$). This means that the intersection is empty if the dimension of the cone $\mathcal{C}$ is less than $m-2$, and otherwise when $\mathcal{C}$ has dimension $m-2, m-1, m$ respectively, the intersection is either empty or it is of dimension $0, 1, 2$ respectively.

With these assumptions, and in particular the transversality assumption, the problem of enumerating the possible phase diagram topologies reduces to understanding the ways in which the pointed secondary fan $\mathcal{F}'(\mathcal{A})$ can decompose an affine 2-dimensional plane inside the $(m-n)$-dimensional space where it lives. It turns out that Gale diagrams hold the key to this problem.

6. Gale diagrams and duality

In this section we introduce Gale diagrams of a vector configuration or affine point configuration, and explain their relationship to (pointed) secondary fans and oriented matroid duality.

Definition 6.1. Given the $n \times m$ matrix $\mathcal{A}$ of rank n whose columns give an affine point configuration, choose a *dual matrix* $\mathcal{A}^*$ to be any $(m-n) \times m$ matrix whose row space $\mathrm{Row}(\mathcal{A}^*)$ coincides with the nullspace (or kernel) $\mathrm{Ker}(\mathcal{A})$. By a similar abuse of notation as in Definition 3.1, the configuration of column vectors $\{a_1^*, \ldots, a_m^*\}$ of this matrix will also be denoted $\mathcal{A}^*$, and is called a *Gale diagram* or *Gale transform* [9] for $\mathcal{A}$. Similarly, we could have started with any $n \times m$ matrix $\mathcal{V}$ of rank n corresponding to a vector configuration and defined a Gale diagram $\mathcal{V}^*$ for it in the same fashion.

Example 6.2. Recall our running example with

$$\mathcal{A} = \begin{array}{c} \begin{matrix} C & D & \frac{1}{2}G & W \end{matrix} \\ \begin{bmatrix} 1 & \frac{1}{2} & \frac{1}{4} & 0 \\ 0 & \frac{1}{2} & \frac{3}{4} & 1 \end{bmatrix} \end{array} \tag{4}$$

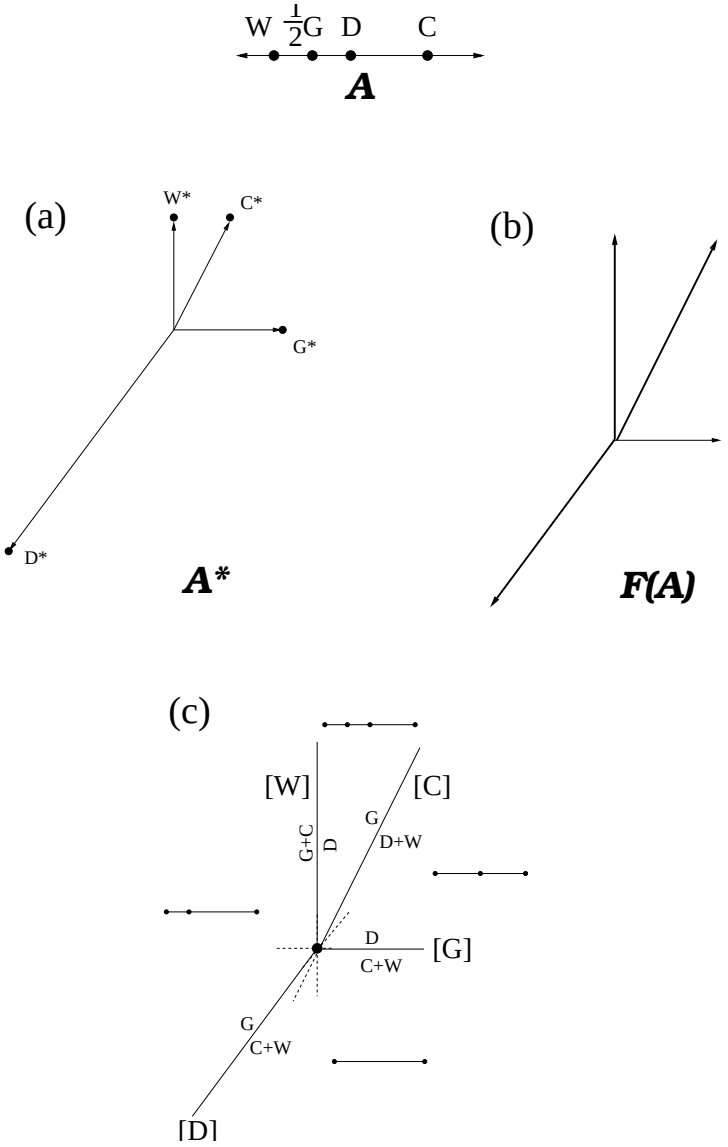

FIGURE 6. (a) Gale diagram $\mathcal{A}^*$, (b) secondary fan $\mathcal{F}(\mathcal{A})$, and (c) invariant point map, for the chemical system corundum-diaspore-gibbsite-water.

An example of a valid Gale diagram for this is

$$\mathcal{A}^* = \begin{matrix} \\ 1 \\ 2 \end{matrix} \begin{matrix} C^* & D^* & G^* & W^* \\ \end{matrix} \begin{bmatrix} 1 & -3 & 2 & 0 \\ 2 & -4 & 0 & 2 \end{bmatrix} \tag{5}$$

and is pictured as a vector configuration in Figure 6.

Note the use of the term "a" Gale diagram, instead of "the" Gale diagram. This is because the rows of $\mathcal{A}^*$ are not uniquely defined: they can be altered by row operations, that is, by the action of $GL_{m-n}(\mathbb{R})$ on the left. This means that the Gale diagram vectors $\mathcal{A}^*$ are also well-defined only up to the same $GL_{m-n}(\mathbb{R})$-action[7].

However, the oriented matroid $\mathcal{M}^*$ associated to the Gale vectors $\mathcal{A}^*$ *is* uniquely defined by the oriented matroid $\mathcal{M}$ associated to $\mathcal{A}$: it is the *dual oriented matroid* [2, §3.4] of $\mathcal{M}$. One manifestation of this duality is that the circuits $\mathcal{C}$ for $\mathcal{A}$ (or $\mathcal{M}$) correspond to sets in $\mathcal{A}^*$ (or $\mathcal{M}^*$) with their own interesting geometric characterization. These sets in $\mathcal{A}^*$ are called cocircuits.

Definition 6.3. Given a configuration of vectors $\mathcal{V} = \{v_1, \ldots, v_m\}$ in $\mathbb{R}^n$, its *covectors* are all possible sign vectors in $\{+, 0, -\}^m$ that can be achieved by evaluating some non-zero linear functional $f \in (\mathbb{R}^n)^*$ on the vectors in $\mathcal{V}$:

$$c = c(f) = (\text{sign}(f(v_1)), \ldots, \text{sign}(f(v_m))$$

A covector c for $\mathcal{V}$ which is maximal with respect to its set of zeroes is called a *cocircuit* of $\mathcal{V}$. Equivalently, a covector is a cocircuit if its corresponding signed subset has minimal support, or equivalently if the subset of $\mathcal{V}$ on which it is 0 contains at least $n-1$ linearly independent vectors. Denote by $\mathcal{C}^*$ the set of cocircuits of $\mathcal{V}$.

As with the circuits $\mathcal{C}$, it is possible to write down a list of *cocircuit axioms* that will be satisfied by the cocircuits $\mathcal{C}^*$ coming from any vector configuration $\mathcal{V}$, and in this way axiomatize the definition of an oriented matroid $\mathcal{M}$ in terms of cocircuits. The observation from above that the circuits C of $\mathcal{A}, \mathcal{V}, \mathcal{M}$ are exactly the cocircuits $\mathcal{C}^*$ of $\mathcal{A}^*, \mathcal{V}^*, \mathcal{M}^*$ means that these cocircuit axioms will look exactly like the circuit axioms.

Example 6.4. In our previous example of $\mathcal{A}$, the first circuit of $\mathcal{A}$ as listed in Example 3.4 was $(0 + -+)$, coming from the reaction $1G \leftrightharpoons$

[7]Recall from Section 3 that there was a similar ambiguity in the definition of the columns of $\mathcal{A}$ or $\mathcal{V}$, stemming from a choice of basis for the space that they span.

$1D + 1W$. In $\mathcal{A}^*$ this is a cocircuit representing the fact that the line spanned by C^* has G^* on one side and D^*, W^* on the opposite side, *i.e.*, there exists a linear functional f for which

$$f(C^*) = 0,\ f(D^*) > 0,\ f(W^*) > 0, \text{ and } f(G^*) < 0.$$

How does the Gale diagram $\mathcal{A}^*$ relate to the pointed secondary fan $\mathcal{F}'(\mathcal{A})$? The relationship comes from looking at the positive cones spanned by the vectors of $\mathcal{A}^*$.

Definition 6.5. Given any set $W = \{w_1, \ldots, w_k\}$ of vectors in $\mathbb{R}^N$, define the *positive cone* spanned by W to be

$$\mathrm{pos}(W) := \left\{ \sum_{i=1}^{k} c_i w_i \in \mathbb{R}^N : c_i > 0 \quad \text{for all } i \right\}.$$

If the set of vectors W happen to be linearly independent, then $\mathrm{pos}(W)$ is called a *(relatively open) simplicial cone*.

Recall that the affine point configuration $\mathcal{A}$ corresponds to an acyclic vector configuration. It is a consequence of oriented matroid duality [2, Proposition 4.8.9] that $\mathcal{A}^*$ will be *totally cyclic*, that is, the origin 0 lies in the cone $\mathrm{pos}(\mathcal{A}^*)$. As a consequence, the collection of positive cones spanned by subsets of $\mathcal{A}^*$ will cover the column space $\mathrm{Col}(\mathcal{A}^*)$, and this covering is closely related to the pointed secondary fan $\mathcal{F}'(\mathcal{A})$:

Theorem 6.6. [3, §4] *The column space* $\mathrm{Col}(\mathcal{A}^*)$ *has a natural identification with the* $(m-n)$*-dimensional subspace complementary to* $\mathrm{Row}(\mathcal{A})$ *within* $\mathbb{R}^m$ *covered by the pointed secondary fan* $\mathcal{F}'(\mathcal{A})$.

Furthermore, under this identification, the cones of $\mathcal{F}'(\mathcal{A})$ *are exactly the common refinement of all the open simplicial cones* $\mathrm{pos}(W)$ *spanned by linearly independent subsets* W *of the Gale (column) vectors* $\mathcal{A}^*$.

One can be more precise about this relationship:

Theorem 6.7. [3, Lemma 4.3] *Given a coherent triangulation* Δ *of* $\mathcal{A}$*, the corresponding* $(m-n)$*-dimensional cone in the secondary fan* $\mathcal{F}'(\mathcal{A})$ *is the intersection*

$$\bigcap_{\sigma \in \Delta} \mathrm{pos}(\mathcal{A}^* - \sigma^*)$$

where here σ *runs through the vertex sets of the* $(n-1)$*-dimensional simplices in the triangulation* Δ*, and*

$$\sigma^* := \{a_i^* : a_i \in \sigma\}.$$

Example 6.8. Because the corundum-diaspore-gibbsite-water example of $\mathcal{A}$ has $m = 4$ and $n = 2$, so that $m = n + 2$, the pointed secondary fan $\mathcal{F}'(\mathcal{A})$ is 2-dimensional. Therefore its top-dimensional cones are simply the sectors between cyclically adjacent Gale vectors in $\mathcal{A}^*$. These cones are depicted in Figure 6(b). In (c) of the same figure, these regions are labelled (as part of the geochemists' invariant point map; see Section 8 below) by their corresponding coherent triangulations.

For example, the sector lying between the Gale vectors W^* and D^* corresponds to a triangulation Δ having two segments $\{GW, CG\}$. This agrees with Theorem 6.7: the complementary sets $\{C^*D^*, D^*W^*\}$ are exactly the ones whose positive cones contain this sector. On the other hand, the sector between between D^*, G^* lies in the positive cone of no other pairs of Gale vectors, and hence corresponds to the triangulation having only one segment, namely the one with vertices $\mathcal{A} - \{D, G\} = \{C, W\}$.

Sections 8 and 9 will closely explore the consequences of the geometry of the Gale diagram for phase diagrams when m is at most $n + 3$. But first we must further explore more general geometric questions.

7. Geometry of the phase diagram in general

In this section we will explain the relationship between Gibbs' phase rule (e.g. [21]) and the secondary fan, and how the phase rule predicts the dimension of various stability fields. We then look closely at the meaning of $2, 1$, and 0-dimensional regions in the phase diagram, relating them to $m, m-1$, and $m-2$-dimensional cones in the secondary fan.

When one fixes particular molar fractions x_i of each of the (rescaled) phases a_i in $\mathcal{A}$ initially contained in a particular sample, the discussion of Section 5 shows how to predict the stable assemblage of phases which will result after allowing the system to find chemical equilibrium. The initial molar fractions give a point $\sum_i x_i a_i = 1$ with $\sum_i x_i = 1$ which lies in the convex hull of $\mathcal{A}$, and lifts to a point $\sum_i x_i \hat{a}_i$ which lies in the convex hull of $\hat{\mathcal{A}}$, but may or may not lie in the *lower* convex hull. After performing reactions which affect the fractions x_i (but preserve the condition $\sum_i x_i = 1$ due to our re-scaling) to reach chemical equilibrium, the lifted point $\sum_i x_i \hat{a}_i$ will evenutally lie in a unique face $\hat{F}$ of the lower hull of $\hat{\mathcal{A}}$. The lifted points $\hat{\mathcal{A}}' \subset \mathcal{A}$ which happen to lie on this face $\hat{F}$ lie above a subset $\mathcal{A}' \subset \mathcal{A}$ of the original phases, that is $\mathcal{A}'$ are those phases which appear with non-zero fraction in this

chemical equilibrium, and $\mathcal{A}'$ labels a polytope F which is part of the corresponding coherent subdivision of $\mathcal{A}$.

Gibbs' phase rule relates three quantities relevant to this situation:

- the number of phases $m' = |\mathcal{A}'| (\leq m = |\mathcal{A}|)$ participating in this chemical equilibrium,
- the number of components $n' (\leq n)$ of the subsystem $\mathcal{A}'$, that is, the dimension of the subspace of chemical composition space spanned by $\mathcal{A}'$, and
- the number of degrees of freedom f in (T, P) which one can vary while maintaining these same phases in equilibrium, or in other words, the dimension of the *union* of all regions in the phase diagram which have $\mathcal{A}'$ labelling one of the polytopes F in their corresponding subdivision of $\mathcal{A}$.

Proposition 7.1. *(Gibbs' phase rule) With the above notations,*

$$f = n' + 2 - m'.$$

In particular, one can have at most $n' + 2$ phases that involve n' components in chemical equilibrium.

Note that in the geochemical literature, the phase rule is often stated as

$$f \leq n + 2 - m',$$

which is consistent with the fact that $n' \leq n$.

Example 7.2. In Figure 1, the triple point has an assemblage of $m' = 3$ phases in equilibria (ice, water, steam), with $n' = 1$ and $f = 0$, while the assemblage consisting of pure ice has $m' = n' = 1$ and $f = 2$.

In Figure 6(c), the line segment DW corresponds to a stable assemblage $\{D, W\}$ in two different divariant regions and the curve that separates them (all in the upper right), so $f = 2$, and it has $m' = n' = 2$. The assemblage $\{D, G, W\}$ is stable only along the univariant curve lying between the two aforementioned divariant regions so $f = 1$, and it has $m' = 3, n' = 2$. The quadruple point in the middle ($f = 0$) of the diagram has all 4 phases in equilibrium, that is, $m' (= m) = 4$, and $n' (= n) = 2$.

We give here a proof of Gibbs' phase rule in terms of the secondary fan $\mathcal{F}(\mathcal{A})$ in $\mathbb{R}^m$.

Proof. There is a cone $\mathcal{C}$ in the secondary fan consisting of those vectors $g \in \mathbb{R}^m$ for which the lifted points $\hat{\mathcal{A}}$ have $\hat{\mathcal{A}}'$ lying on a face $\hat{F}$ of the lower hull: this cone is the intersection of the vector space V on which the lifted points $\hat{\mathcal{A}}'$ all lie on a single n'-dimensional affine subspace

with the half-spaces given by various inequalities that assert all the other lifted points $\hat{a}_i$ in $\mathcal{A} - \mathcal{A}'$ lift *above* this affine subspace. The subspace V is defined by $m' - n'$ linear conditions: after choosing the height coordinates of g to lift n' of the elements $\mathcal{A}'$ which are affinely independent, the remaining $m' - n'$ coordinates of must be lifted to heights which are linear functions of those first n' heights. Thus V has dimension $m - (m' - n')$. The fact that lifting all the points $\mathcal{A} - \mathcal{A}'$ to any sufficiently large heights will force $\hat{F}$ to be in the lower hull shows that the cone $\mathcal{C}$ obtained by intersecting V with the various half-space inequalities will have the same dimension as V, namely $m - (m' - n')$.

By Proposition 5.3 and Assumption 5.4, the union of all regions in the phase diagram which have $\mathcal{A}'$ labelling one of the polytopes F in their corresponding subdivision of $\mathcal{A}$ comes from the the transverse intersection of an affine 2-plane with the cone $\mathcal{C}$. If $m' - n' > 2$, there would be no intersection due to Assumption 5.4. If $m' - n' \leq 2$, then since we assumed that these phases $\mathcal{A}'$ could exist in stable equilibrium, there must be a non-empty intersection. Depending upon whether $m' - n' = 0, 1$, or 2, this transverse intersection of $\mathcal{C}$ with an affine 2-plane will have dimension $f = 2, 1$, or 0 respectively, i.e. $f = 2 - (m' - n') = n' + 2 - m'$. □

Understanding the $2, 1$, and 0-dimensional regions in the phase diagram amounts to understanding the cones of dimensions $m, m-1$, and $m-2$ in the secondary fan $\mathcal{F}(\mathcal{A})$ or equivalently, the cones of dimensions $m-n, m-n-1, m-n-2$ in the pointed secondary fan $\mathcal{F}'(\mathcal{A})$. The 2-dimensional regions in the phase diagram correspond to the top-dimensional cones in $\mathcal{F}(\mathcal{A})$ (or $\mathcal{F}'(\mathcal{A})$), which are labelled by the coherent triangulations of $\mathcal{A}$ in the manner described in Theorem 6.7, and there is little to add to that description. The more interesting cases are those of the 1 and 0 dimensional stability fields.

7.1. **Bistellar operations and 1-dimensional stability fields.** The 1-dimensional curves separating the regions in the phase diagrams correspond to natural transformations on triangulations of $\mathcal{A}$ called *bistellar operations*, that are closely related to the circuits of $\mathcal{A}$. We discuss these now somewhat informally; for a more formal treatment, see [10, Chapter 7 §2C].

Figure 7 illustrates three examples of a pair of triangulations of affine point configurations $\mathcal{A}$ in $\mathbb{R}^2$ that are related by a bistellar operation. For each bistellar operation between two triangulations, there is a distinguished subset $C \subset \mathcal{A}$ which is the support set $C = X^+ \cup X^-$ of some signed circuit (X^+, X^-) of $\mathcal{A}$, and such that the convex hull of

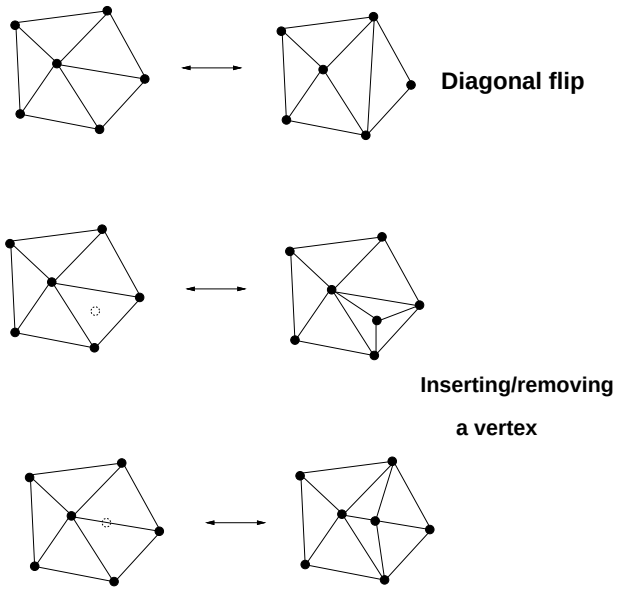

FIGURE 7. Three examples of pairs of bistellar operations for triangulations of affine point configurations $\mathcal{A}$ in $\mathbb{R}^2$.

C is triangulated (differently!) in the two triangulations. In this case, we say that the bistellar operation is *supported on the circuit* C. Note that in the first two examples in Figure 7 this circuit C has a full 2-dimensional convex hull, but as the third example illustrates, C can have a convex hull of lower dimension.

Recall that a circuit $C = X^+ \cup X^-$ of $\mathcal{A}$ corresponds to a cocircuit of $\mathcal{A}^*$, that is there is an $(m-n-1)$-dimensional hyperplane H_C spanned by the Gale vectors indexed by $\mathcal{A} - C$ which separates the Gale vectors indexed by X^+ from those indexed by X^-. When C is the circuit supporting a bistellar operation between two triangulations, this reflects the following geometry of pointed secondary fans.

Proposition 7.3. [10, §7.2.C] *Two triangulations* Δ, Δ' *differ by a bistellar operation supported on a signed circuit* C *if and only if their corresponding top dimensional cones in* $\mathcal{F}'(\mathcal{A})$ *are adjacent along a wall whose linear span is the hyperplane* H_C.

This has an interpretation for the temperature pressure phase diagram which is well-known to geochemists: the segments of curves separating regions in the phase diagram are always portions of a larger curve corresponding to some minimal reaction possible among the phases in the chemical system. Two regions will be adjacent and separated by such a curved segment if and only if their corresponding triangulations differ by retriangulating the convex hull of the phases involved in that reaction.

It is also useful to think of a bistellar operation as represented by the coherent polytopal subdivision that labels the wall between the two top dimensional cones guaranteed by the previous proposition. In the language of Gibbs' phase rule, this subdivision contains a special polytopal face F labelled by a subset $\mathcal{A}' \subset \mathcal{A}$ having $m' = n' + 1$; namely $\mathcal{A}'$ is the support set of the circuit C. Note that if $n' = n$ then F is a full $(n-1)$-dimensional polytope in the subdivision, and all the other full-dimensional polytopes in the subdivision are $(n-1)$-dimensional simplices.

A reasonable question at this point is, "How well do the bistellar operations tie together the set of all triangulations of $\mathcal{A}$— is it possible to connect any two triangulations of a point set $\mathcal{A}$ by a sequence of bistellar operations?" The answer has important consequences for calculating the set of triangulations of $\mathcal{A}$: the algorithms (e.g. [20]) that start with one triangulation and find the rest bistellarly connected to it by performing all possible bistellar operations are much faster than algorithms that find *all* triangulations by the currently available techniques [7, 20].

Unfortunately, the answer to the above question is "No" in general: Santos [22, 23] has recently produced examples of triangulations of affine point configurations that are connected to *no* other triangulations (!) by bistellar operations. Fortunately, however there are positive results relevant for the geochemical applications:

- All triangulations are connected by bistellar operations when $n \leq 3$ [14],
- the same holds when $m - n \leq 3$ [1], and
- the subset of *coherent* triangulations are always connected by bistellar operations [10].

In particular, this last result allows one to rely on the very fast bistellar flip algorithms of [20] (utilized in [18]) to find all of the coherent triangulations.

7.2. **Invariant points and indifferent crossings.** We conclude this section with an informal discussion of 0-dimensional regions in the

phase diagram. These will correspond to cones of dimension $m-2$ in $\mathcal{F}(\mathcal{A})$ or cones of dimension $m-n-2$ in $\mathcal{F}'(\mathcal{A})$. These correspond to coherent polytopal subdivisions of $\mathcal{A}$ of two possible types, and therefore give rise to two distinct types of points in the phase diagram: invariant points and indifferent crossings.

Definition 7.4. If a coherent polytopal subdivision of $\mathcal{A}$ corresponds to a cone of dimension $m-2$ in $\mathcal{F}(\mathcal{A})$, then one of the polytopes F' in the subdivision might correspond to a stable assemblage $\mathcal{A}'$ having $m' = n'+2$ phases. When this occurs, the same holds for every polytope in the subdivision which contains F' as a face. However, the remaining polytopes which do not contain F' will all be simplices.

It is in this situation that geochemists reserve the term *invariant point* for the corresponding 0-dimensional region in the phase diagram. In this situation it is possible for all of the phases in $\mathcal{A}'$ to co-exist in chemical equilibrium, but one cannot vary (T, P) at all while maintaining this. For example, the central point in Figures 1 and 6(c) are invariant points, as are the points labelled $[B], [C], [D], [G], [W]$ within the diagrams labelling regions in Figure 12.

Geochemists usually label the invariant point by the phases $\mathcal{B} := \mathcal{A} - \mathcal{A}'$ *not* involved in the invariant equilibrium. It is also well-known to geochemists that the local structure of the phase diagram around an invariant point is similar to the corresponding phase diagram with $m' = n' + 2$ for the chemical subsystem $\mathcal{A}'$. This corresponds to the known fact [4] that the local structure of the pointed secondary fan $\mathcal{F}'(\mathcal{A})$ about the cone $\mathrm{pos}(\mathcal{B})$ and the structure of the fan $\mathcal{F}'(\mathcal{A}') = \mathcal{F}'(\mathcal{A} - \mathcal{B})$ coincide, reflecting the fundamental duality between *deletion* and *contraction* in (oriented) matroid theory: the dual point configuration $(\mathcal{A}-\mathcal{B})^*$ to the deletion $\mathcal{A}-\mathcal{B}$ is isomorphic to the contraction $\mathcal{A}^*/\mathcal{B}^*$.

Definition 7.5. On the other hand, when a cone in $\mathcal{F}(\mathcal{A})$ has dimension $m-2$, there can also be two polytopes F' and F'' in the corresponding polytopal subdivision, neither contained as a face of the other, corresponding to stable assemblages $\mathcal{A}'$ and $\mathcal{A}''$ with $m' = n'+1, m'' = n''+1$. The polytopes in the subdivision containing neither of F' or F'' will all be simplices. For each of $\mathcal{A}'$ or $\mathcal{A}''$ individually, the union of regions in the phase diagram where they occur as a stable assemblage corresponds to a cone of dimension $m-1$ in $\mathcal{F}(\mathcal{A})$, and a curve in the phase diagram coming from a minimal reaction possible in $\mathcal{A}$. These two curves intersect at what is called an *indifferent crossing*, where either $\mathcal{A}'$ or $\mathcal{A}''$ might exist in equilibrium (as might assemblages corresponding to other simplices in the subdivision), but the union $\mathcal{A}' \cup \mathcal{A}''$

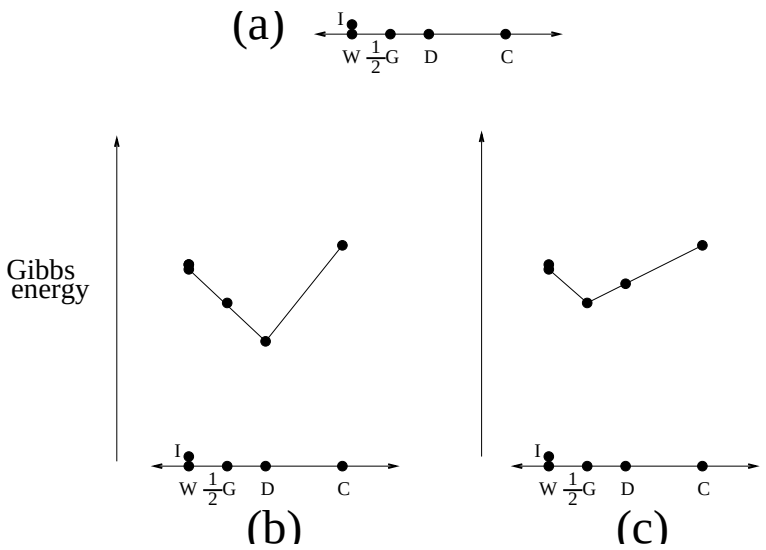

FIGURE 8. An $m = n + 3$ system illustrating the distinction between invariant points and indifferent crossings.

cannot stably co-exist: the faces F', F'' lift to two different faces in the lower hull of $\hat{\mathcal{A}}$, lying above disjoint possibilities for the molar fractions of the phases.

Example 7.6. To illustrate the distinction between the two kinds of cones of dimension $m - 2$ in $\mathcal{F}(\mathcal{A})$ that give rise to invariant points versus indifferent crossings, we augment our previous chemical system of corundum, diaspore, gibbsite, water with a fifth phase: ice, abbreviated I, having chemical formula H_20, the same as water. Rescaling this to a chemography as before gives a new chemography $\mathcal{A}$ with $n = 2$ as before, but now with $m = 5 = n + 3$, depicted in Figure 8(a). Figures 8(b) and (c) depict lifted configurations $\hat{\mathcal{A}}$ that would correspond to cones of dimension $(m - 2)$ in $\mathcal{F}(\mathcal{A})$ corresponding to an invariant point and indifferent crossing, respectively.

In (b), the interesting stable assemblage is $\mathcal{A}' = \{D, G, W, I\}$ having $m' = 4, n'(= n) = 2$ so $m' = n' + 2$, and the corresponding lifted points $\hat{\mathcal{A}}'$ lie on a single face F' in the lower hull of $\hat{\mathcal{A}}$. If the phase diagram

were to contain a point corresponding to this cone of $\mathcal{F}(\mathcal{A})$, it would be an invariant point, labelled $[C]$ for the missing phase corundum not in $\mathcal{A}'$.

In (c), there are at least two interesting stable assemblages: $\mathcal{A}' = \{W, I\}$ with $m' = 2, n' = 1$, and $\mathcal{A}'' = \{C, D, G\}$ with $m'' = 3, n' = 2$, so that $m' = n' + 1, m'' = n'' + 1$, and their corresponding lifted points $\hat{\mathcal{A}}', \hat{\mathcal{A}}''$ span different faces F', F'' of the lower hull of $\hat{\mathcal{A}}$. If the phase diagram were to contain a point corresponding to this cone of $\mathcal{F}(\mathcal{A})$, it would be an indifferent crossing, lying at the intersection of two curves corresponding to the two circuits (reactions) involving the phases $\mathcal{A}'$ and $\mathcal{A}''$.

8. The case $m = n + 2$: phase diagram = Gale diagram

After dispensing quickly with the cases $m = n$ and $m = n + 1$, in this section we examine in detail the structure of Gale diagram $\mathcal{A}^*$, the pointed secondary fan $\mathcal{F}'(\mathcal{A})$, and the phase diagram when $m = n+2$. The conclusion is that they all look roughly the same in this case.

When $m = n$, the m phases cannot perform any reactions that preserve mass-balance, and so are mutually inert and nothing can happen.

When $m = n + 1$, not much interesting happens. There is exactly one reaction possible, corresponding to the unique signed circuit $C = (X^+, X^-)$ of $\mathcal{A}$. The Gale diagram $\mathcal{A}^*$ is a set of vectors lying on the real line $\mathbb{R}^1$ with their tails at the origin 0. Those a_i^* having $i \in X^+$ will point in the positive direction, those with $i \in X^-$ will point in the negative direction, and those $i \in \{1, \ldots, m\} - (X^+ \cup X^-)$ will be zero vectors pointing nowhere. The secondary fan $\mathcal{F}'(\mathcal{A})$ decomposes the $\mathbb{R}^1$ into two cones: the two rays emanating from the origin in the positive and negative directions. These rays correspond to the two triangulations of $\mathcal{A}$ which differ by a bistellar operation supported on C. At a particular temperature and pressure, the Gibbs energy of the ensemble of products/reactants, whichever is lower, will force the reaction to run in one direction or another, so that the stable assemblages will correspond to the simplices of one or the other triangulation. In this case, the phase diagram consists of two divariant regions separated by the univariant curve corresponding to the single reaction.

When $m = n + 2$, things start to become interesting. First, we can assume without loss of generality that there are no *indifferent phases*[8], that is, every phase participates in some possible reaction or phase

[8]An indifferent phase would give rise to an element a_i of the oriented matroid for $\mathcal{A}$ known as an *isthmus* or *coloop*, and also to a zero Gale vector $a_i^* = 0$.

change. By excluding indifferent phases, we know that the Gale diagram $\mathcal{A}^*$ has m non-zero Gale vectors $a_1^*, \ldots, a_m^*$, although it is possible that some differ by positive scalar multiples and hence point in the same direction[9]. The pointed secondary fan $\mathcal{F}'(\mathcal{A})$ will look very similar to the Gale diagram, having at most m rays emanating from the origin, pointing in the directions of the Gale vectors, and 2-dimensional cones lying between cyclically adjacent Gale vectors. According to Proposition 5.3, the phase diagram should look roughly like a 2-dimensional slice of this 2-dimensional pointed secondary fan $\mathcal{F}'(\mathcal{A})$, that is, like $\mathcal{F}'(\mathcal{A})$ itself. Hence the phase diagram will closely resemble the Gale diagram $\mathcal{A}^*$.

Roughly speaking, geochemists have known some version of this, in the guise of a method for constructing their *invariant point maps* as schematic representations of the local picture around an invariant point, based on knowledge of the minimal reactions possible among the phases. Their method uses Schreinemakers' *fundamental axiom* [25, 30], which is a re-formulation of the oriented matroid duality assertion that the circuits of $\mathcal{A}$ coincide with the cocircuits of $\mathcal{A}^*$. The axioms assert that

- each phase a_i should label some univariant reaction half-line emanating from the invariant point, corresponding to a minimal reaction among the remaining phases other than a_i, and
- the extension of this half-line to a line through the origin should separate the other univariant reaction half-lines into those corresponding to the two sides of the reaction in question.

In other words, each Gale vector a_i^* lies on a line through the origin corresponding to a cocircuit of $\mathcal{A}^*$, which corresponds to a circuit of $\mathcal{A}$.

Using this rule, one can sketch the invariant point map by proceeding through the list of minimal reactions among the phases, and using the axiom to place the half-lines around each other in cyclic order. There is an initial choice of orientation one must make for the diagram using the first reaction (should the reactant/products/missing-phase-half-line go in *clockwise* or *counterclockwise* order around the invariant point?), but after that the picture is determined. To decide which orientation is consistent with the actual geochemical phase diagram (i.e. to determine the actual placement of the image surface $\gamma(\mathbb{R}^2)$ within the secondary fan $\mathcal{F}(\mathcal{A})$), some thermodynamic data is required.

[9]This will happen whenever there are affine hyperplanes in $\mathbb{R}^{n-1}$ that contain all but two of the points of $\mathcal{A}$

Example 8.1. Figure 6(c) shows the invariant point map constructed for the corundum-diaspore-gibbsite-water example. Note that we have used the geochemical conventions of labelling the univariant reaction half-lines emanating from the invariant point by the phase(s) missing from the reaction, putting the product/reactants on either side of the line, and indicating with dashes the *metastable* extensions of these half-lines.

9. The case $m = n + 3$: phase diagram = affine Gale diagram

We next examine in detail the structure of the Gale diagram $\mathcal{A}^*$, the pointed secondary fan $\mathcal{F}'(\mathcal{A})$, and the phase diagram when $m = n+3$. The conclusion is that two methods used by geochemists to reduce an essentially 3-dimensional picture to two dimensions have parallel constructions in discrete geometry, and the phase diagram bears a close resemblance to a 2-dimensional affine Gale diagram.

When $m = n + 3$, we can again assume without loss of generality that there are no indifferent phases, and hence no zero Gale vectors a_i^*. However we make no other genericity assumptions for the moment. The Gale diagram $\mathcal{A}^*$ is a vector configuration in $\mathbb{R}^3$. As before, some Gale vectors may differ by a positive scalar multiple and hence give rise to the same ray in the secondary fan $\mathcal{F}'(\mathcal{A})$, so we know there will be at most m such rays. Note that unlike the case $m = n + 2$, here the cones of the pointed secondary fan $\mathcal{F}'(\mathcal{A})$ can be more exotic in shape: they are intersections of the 3-dimensional simplicial cones spanned by linearly independent subsets of $\mathcal{A}^*$, and hence can have arbitrary polygonal cross-sections.

The one-dimensional cones (rays) in $\mathcal{F}'(\mathcal{A})$ will correspond to 0-dimensional (point) regions in the phase diagram when they intersect the image surface $\gamma(\mathbb{R}^2)$ of the Gibbs energy map. As discussed in Subsection 7.2, these points will either be indifferent crossings or invariant points. Since the invariant points correspond to chemical subsystems $\mathcal{A}' \subset \mathcal{A}$ which have $m' = n' + 2$, if we have $n' = n$ (as happens generically) then $|\mathcal{A}'| = |\mathcal{A}| - 1$, that is, there is exactly one phase a_i missing from $\mathcal{A}'$, and the corresponding ray in $\mathcal{F}'(\mathcal{A})$ is spanned by the Gale vector a_i^*. This is the reason that invariant points in phase diagrams with $m = n + 3$ are generically labelled by the single phase missing from the invariant equilibrium at that point. As also discussed in Subsection 7.2, the local structure about the invariant point will look like the invariant point map for the $m' = n' + 2$ subsystem $\mathcal{A}'$.

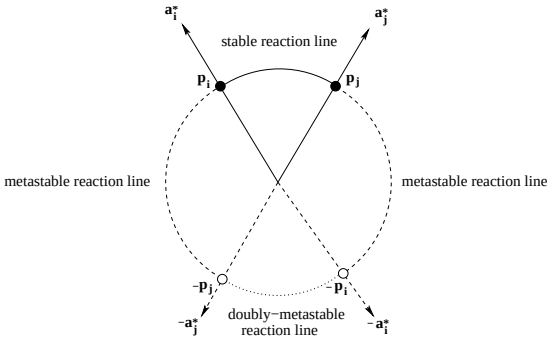

FIGURE 9. A typical reaction loop defined by two Gale vectors $\mathbf{a}_i^*$ and $\mathbf{a}_j^*$.

Vector configurations in $\mathbb{R}^3$ (like $\mathcal{A}^*$) can be difficult to visualize. We discuss two methods that have been commonly used to cut down the dimension by one (and produce a picture closer in spirit to the phase diagram): the *spherical representation* and *affine Gale diagrams*.

9.1. **The spherical representation: closed nets.** Intersecting the pointed secondary fan $\mathcal{F}'(\mathcal{A})$ in $\mathbb{R}^3$ with a unit sphere centered about the origin gives a useful spherical representation, similar to what has been called a *closed net* in [29]. In the conventions for the closed net, one includes not only the point of intersection with the sphere $p_i := \frac{a_i^*}{|a_i^*|}$ for each ray spanned by a Gale vector a_i^* (represented by a black dot labelled by the corresponding phase a_i), but also its negation $-p_i$ (represented by a white dot labelled similarly)[10]. Furthermore, the arc representing the intersection curve on the sphere of a 2-dimensional cone in $\mathcal{F}'(\mathcal{A})$ is augmented to be part of a great circle called a *reaction loop*, corresponding to the unique minimal reaction (circuit of $\mathcal{A}$, cocircuit of $\mathcal{A}^*$) to which it is associated. Typically such a reaction will involve all but two phases a_i, a_j (although this will not always be the case when $\mathcal{A}$ is not generic and therefore has some circuits of smaller

[10]This supplementation of the Gale diagram $\mathcal{A}^*$ by adding in negations of all its vectors is reminiscent of the *Lawrence construction* [2, §9.3] in oriented matroid theory.

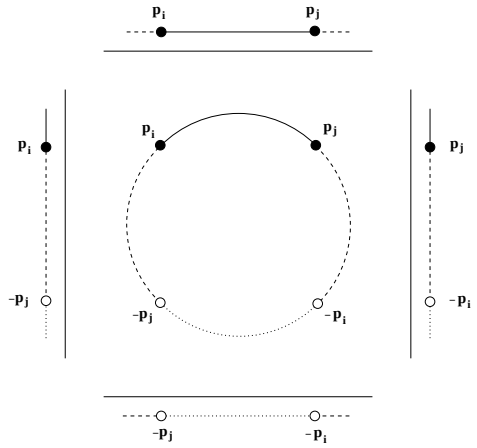

FIGURE 10. The four possible projections of a reaction loop onto an affine 2-plane.

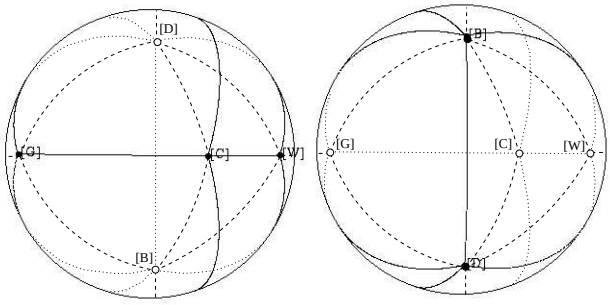

FIGURE 11. Two opposing hemispheric views of the closed net for the system with phases corundum, boehmite, diaspore, gibbsite, and water.

support). As one traverses such a typical reaction loop, one passes through four arcs as depicted in Figure 9.

The point of the closed net representation is that a hemispherical or planar projection of it from some angle should give a schematic picture of the actual phase diagram. Which projection occurs in nature will depend upon the location and orientation of the image surface $\gamma(\mathbb{R}^2)$ of the Gibbs energy map from Section 5 inside the secondary fan $\mathcal{F}(\mathcal{A})$. Under our Assumption 5.4, one of each pair $\{p_i, -p_i\}$ will appear in the projection, and there are four possibilities for the portion of a typical reaction loops that will appear in the projection, depicted in Figure 10.

Example 9.1. We add a fifth phase (different from the ice added in Example 7.6) to our original example of corundum, diaspore, gibbsite, and water: the mineral *boehmite* (B) which is a *polymorph* of diaspore, that is, it has the same chemical formula $AlO(OH)$, but different crystal structure. Thus B, D become parallel elements in the oriented matroid $\mathcal{M}$ for this new point configuration $\mathcal{A}$, having $m = 5$ and $n = 2$, so that $m = n + 3$.

We have

$$\begin{array}{c} \\ \mathcal{A} = \end{array} \begin{array}{c} \begin{array}{ccccc} C & D & B & \frac{1}{2}G & W \end{array} \\ \begin{bmatrix} 1 & \frac{1}{2} & \frac{1}{2} & \frac{1}{4} & 0 \\ 0 & \frac{1}{2} & \frac{1}{2} & \frac{3}{4} & 1 \end{bmatrix} \end{array} \tag{6}$$

and a valid Gale transform is

$$\begin{array}{c} \\ \mathcal{A}^* = \end{array} \begin{array}{c} \begin{array}{ccccc} C^* & D^* & B^* & G^* & W^* \end{array} \\ \begin{bmatrix} 1 & 0 & 0 & -4 & 3 \\ 0 & 1 & 0 & -2 & 1 \\ 0 & 0 & 1 & -2 & 1 \end{bmatrix} \end{array} \tag{7}$$

Two opposite hemispheric views of the closed net for this example are depicted in Figure 11. Note that the parallel elements B, D in $\mathcal{A}$ give rise to a circuit

$$\begin{array}{ccccc} C & D & B & G & W \\ 0 & + & - & 0 & 0 \end{array}$$

that corresponds to a cocircuit of $\mathcal{A}^*$: the Gale vectors C^*, G^*, W^* are coplanar, and their corresponding points on the closed net lie on a great circle which separates D^* from B^*.

9.2. **Two-dimensional affine Gale diagrams.** The affine Gale diagram is simply an affine point configuration in $\mathbb{R}^2$ used to encode the 3-dimensional vector configuration $\mathcal{A}^*$; see [33, Definition 6.17], [2,

§9.1]. Arbitrarily choose a 2-dimensional affine plane Γ in $\mathbb{R}^3$ to "slice" the Gale vectors: if this plane Γ is defined by the equation $f(x) = c$ for some generic linear functional $f \in (\mathbb{R}^3)^*$ and some positive value c, then we replace each Gale vector a_i^* by the unique point $c\frac{a_i^*}{f(a_i^*)}$ in its span that lies in this plane Γ. Color these rescaled Gale points in Γ black or white depending upon whether $f(a_i^*) > 0$ or $f(a_i^*) < 0$. Since $\mathcal{A}$ was an affine point configuration and hence $\mathcal{A}^*$ is a totally cyclic vector configuration, there will always be both black and white points in the affine Gale diagram, regardless of how the functional f is chosen.

We can further annotate the affine Gale diagram by drawing in line segments that correspond to the intersections of 2-dimensional cones from $\mathcal{F}'(\mathcal{A})$ with the plane Γ that happen to connect the black points in the diagram. Bearing in mind Assumption 5.4, the choice of the functional f (equivalently, the choice of the plane Γ) corresponds to the choice of the location of the image surface $\gamma(\mathbb{R}^2)$ of the Gibbs energy map. It follows from Proposition 5.3 that this "decorated affine Gale diagram" is a schematic picture for one possible toplogy of the phase diagram. Such schematic pictures, when annotated further with more arcs of reaction loops using conventions similar to the closed nets discussed in Subsection 9.1 above, have appeared in [17] and are called *potential solutions* for the phase diagram topology.

When are two such affine Gale diagrams/potential solutions considered "equivalent"? Fortunately, discrete geometers and geochemists agree on this: when the assignment of either a black and white dot to each phase is the same. Equivalently, this means they have the same sign vector $(\text{sign}(f(a_1^*)), \ldots, \text{sign}(f(a_m^*)) \in \{+, -\}^m$, or in oriented matroid terminology, that f achieves the same *acyclic (re-)orientation* (or *tope*) of the vector configuration $\mathcal{A}^*$ [2, Section 3.8]. This turns out to have the following geometric re-intepretation: if we regard the functional $f(x) = f_1x_1 + f_2x_2 + f_3x_3$ as its vector of coefficients (f_1, f_2, f_3), then the acyclic orientation achieved by f is determined by which side of each of the hyperplanes $(a_i^*)^\perp$ normal to the Gale vectors it lies on. Therefore intersecting this arrangement of hyperplanes $(a_i^*)^\perp$ with the unit sphere in $\mathbb{R}^3$ gives an arrangement of great circles on the sphere (called the *Euler sphere* in [16]), whose 2-dimensional regions parametrize the different acyclic orientations/affine Gale diagrams/potential solutions.

The method developed in [16] of constructing potential solutions for systems with $m = n + 3$ systems involved looking at each phase, using the method of Schreinemaker from Section 8 to infer the local structure/invariant point map about the invariant point where that

phase is missing from the assemblage, and then "fitting together" these various invariant point maps to produce the straight line net.

Example 9.2. Figure 12 shows a view of the Euler sphere for the previous example with $m = n+3$, along with two of its regions labelled by their corresponding affine Gale diagrams/potential solutions.

There is a good bit of theory to help one enumerate these acyclic reorientations (see [2, Theorem 4.6.1] and Subsection 10.2 below), or to produce a list of them all algorithmically using a straightforward application of Farkas' lemma [26, §7.3]. In the Java applet "CHEMOGALE" [18], such an algorithm is part of the implementation. For systems input by the user with $m = n + 2$ or $n + 3$, the program computes $\mathcal{A}^*$ and uses data generated by [20] to obtain $\mathcal{F}'(\mathcal{A})$. When $m = n + 3$, the intersection of $\mathcal{F}'(\mathcal{A})$ with the unit sphere is depicted, allowing the user to select 2-dimensional cones of $\mathcal{F}'(\mathcal{A})$ and receive the corresponding triangulation. For $m = n+3$ systems, the user may also view the Euler sphere and see the potential solution to the phase diagram topology associated with each region. This work was fully described in [19, Chapter 3].

10. Further implications/applications

We collect here a few further implications/applications of some of the theory developed.

10.1. **Slopes around invariant points.** Let p be an invariant point in the phase diagram, and let $\{a_1, \ldots, a_k\}$ be the union of all sets of phases that can form stable assemblages at p. There will be at most k univariant reaction curves emanating from p corresponding to reactions that omit each of the phases a_i, and each has a limiting slope μ_i as it enters p. Doing the experiments to determine these slopes accurately is expensive and time-consuming, so it is helpful to be able to determine the slopes from as little data as possible.

Proposition 10.1. *Knowing the formulae $\{a_1, \ldots, a_k\}$ of the phases, and knowing three different limiting slopes $\mu_{i_1}, \mu_{i_2}, \mu_{i_3}$ determines all of the slopes $\mu_1, \ldots, \mu_k$.*

Proof. As discussed in Section 7.2, the local structure of the phase diagram about p coincides with the phase diagram for only the subsystem of phases in $\mathcal{A}' := \{a_1, \ldots, a_k\}$, and this must be a system with $k = n + 2$ phases. Let its Gale transform be $\mathcal{A}'^* := \{a_1^*, \ldots, a_k^*\}$, so that up to an invertible linear change-of-basis in $\mathbb{R}^2$, these give the slopes of the rays emanating from the origin in the pointed secondary

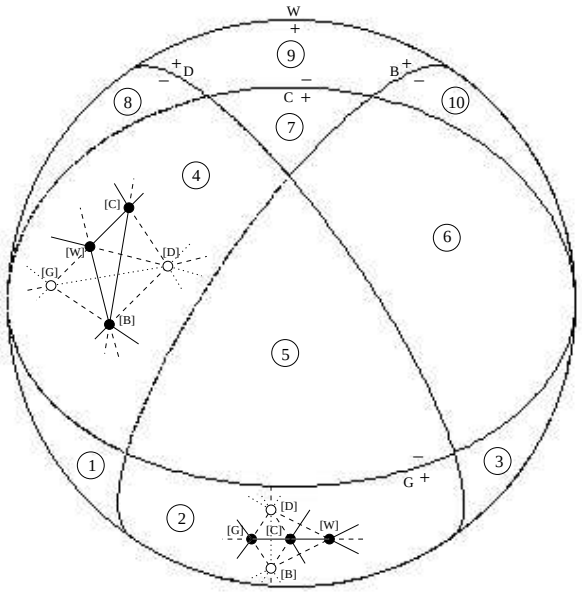

FIGURE 12. The hemisphere of the Euler sphere lying in one side of $(W^*)^\perp$ for the $m = n + 3$ system with phases corundum, boehmite, diaspore, gibbsite, and water. Two regions are shown labelled by the corresponding affine Gale diagrams/potential solutions to phase diagram topology.

fan $\mathcal{F}'(\mathcal{A}')$. By Assumption 5.4, the slopes $\{\mu_1, \ldots, \mu_k\}$ are also related to the slopes of these rays in the pointed secondary fan by an invertible linear change-of-basis (namely, the Jacobian matrix of the Gibbs energy map $\gamma : \mathbb{R}^2 \to \mathbb{R}^m$ evaluated at the point $p \in \mathbb{R}^2$, composed with the linear projection map from $\mathbb{R}^m \to \mathbb{R}^{m-n}$ that sends the secondary fan to the pointed secondary fan). Hence the (known) slopes of the Gale vectors in $\mathcal{A}'^*$ are related to the limiting slopes about p by an invertible linear change-of-basis. Therefore knowledge of 3 distinct slopes $\mu_{i_1}, \mu_{i_2}, \mu_{i_3}$ will determine any other slope μ_{i_r}, e.g. by invariance

under invertible linear transformations of the *cross-ratio*

$$(\mu_{i_1}, \mu_{i_2} \mid \mu_{i_3}, \mu_{i_r}) := \frac{(\mu_{i_r} - \mu_{i_1})(\mu_{i_3} - \mu_{i_2})}{(\mu_{i_r} - \mu_{i_2})(\mu_{i_3} - \mu_{i_1})}.$$

□

Example 10.2. In the example of corundum, diaspore, gibbsite, and water, which had Gale diagram

$$\mathcal{A}^* = \begin{matrix} \\ \end{matrix} \begin{matrix} C^* & D^* & G^* & W^* \end{matrix} \\ \begin{bmatrix} 1 & -3 & 2 & 0 \\ 2 & -4 & 0 & 2 \end{bmatrix} \tag{8}$$

we see that the slopes of C^*, D^*, G^*, W^* are $2, \frac{4}{3}, 0, \infty$ giving the cross-ratio

$$(\mu_{C^*}, \mu_{G^*} \mid \mu_{W^*}, \mu_{D^*}) = \frac{(\frac{4}{3} - 2)(\infty - 0)}{(\frac{4}{3} - 0)(\infty - 2)} = -\frac{1}{2}.$$

Thus if we have already determined (say from thermodynamic data) that the phase diagram has limiting slopes $\mu_{[C]}, \mu_{[G]}, \mu_{[W]}$ for the three reaction curves labelled $[C], [G], [W]$ entering the invariant point, then the limiting slope $\mu_{[D]}$ of the fourth reaction curve labelled $[D]$ will satisfy

$$-\frac{1}{2} = (\mu_{[C]}, \mu_{[G]} \mid \mu_{[W]}, \mu_{[D]}) = \frac{(\mu_{[D]} - \mu_{[C]})(\mu_{[W]} - \mu_{[G]})}{(\mu_{[D]} - \mu_{[G]})(\mu_{[W]} - \mu_{[C]})}$$

which can be solved for $\mu_{[D]}$, giving the formula

$$\mu_{[D]} = \frac{3\mu_{[C]}\mu_{[G]} - 2\mu_{[C]}\mu_{[W]} - \mu_{[G]}\mu_{[W]}}{2\mu_{[G]} - 3\mu_{[W]} + \mu_{[C]}}.$$

10.2. **Counting potential solutions.** As mentioned in Section 9.2, there is theory available for counting the acyclic orientations of a vector configuration (or oriented matroid) such as the Gale diagram $\mathcal{A}^*$. Here we elaborate on this and explain how to easily count potential solutions to phase diagram topology when $m = n + 3$.

As we saw in Section 9.2, counting the potential solutions to phase diagram topology amounts to counting the 3-dimensional cones cut out by an arrangement of planes through the origin in $\mathbb{R}^3$, or the 2-dimensional regions cut out by an arrangement of great circles on a sphere, or the acyclic orientations of the oriented matroid $\mathcal{M}^*$ associated to the Gale diagram $\mathcal{A}^*$. The problem of counting the n-dimensional regions cut out by an arrangement of $(n-1)$-dimensional hyperplanes through the origin in $\mathbb{R}^n$ was treated first by Winder in 1966, and then later independently by both Las Vergnas and Zaslavsky

around 1975. The basic idea is that even though the combinatorial structure of the regions cut out (e.g. how many faces of each dimension they have) depends on the associated *oriented* matroid, the number of regions only depends up the coarser information recorded in the *matroid*. We review some of this material here; see [2, §4.6] for a fuller treatment.

For example, one way to record the matroid data associated to $\mathcal{A}^*$ is to list all of its (unsigned) *circuits*, which are the support sets of minimal linear dependences (with no record of the signs of the coefficients in the dependence). An alternative way to encode the data which is more useful for counting the regions (but equivalent data to specifying the circuits) is to write down the *lattice of flats* $L(\mathcal{A}^*)$, which is the partial ordering by inclusion of all subspaces spanned by subsets of $\mathcal{A}^*$. The bottom element of this partially ordered set, called $\hat{0}$, corresponds to the zero subspace (spanned by the empty set of Gale vectors).

The *Möbius function* $\mu(x, y)$ is an integer associated to each pair of elements $x \leq y$ which are related in the partial order L, defined recursively by these properties:

$$\mu(x, x) = +1$$
$$\mu(x, y) = -\sum_{x \leq z < y} \mu(x, z) \text{ if } x < y.$$

One can use this to count regions via the following result.

Theorem 10.3. [2, Theorem 4.6.1] *The number of regions cut out by the hyperplanes normal to a collection of vectors with lattice of flats L is*

$$\sum_{x \in L} |\mu(\hat{0}, x)|.$$

Since we wish to apply this is to geochemical systems with $m = n+3$, we detail here explicitly (in more concrete terms) what happens in this case.

Proposition 10.4. *Let $\mathcal{A}$ be a chemography with $m = n+3$, so that its Gale diagram $\mathcal{A}^*$ is a configuration of vectors in $\mathbb{R}^3$. Then the number of potential solutions to phase diagram topology is*

$$2\left(1 + \sum_{P} (m_P - 1)\right)$$

where P runs through all 2-dimensional planes spanned by pairs of the Gale vectors $\mathcal{A}^*$, and m_P is the number of distinct lines spanned by Gale vectors lying in the plane P (or equivalently, the number of parallelism classes of Gale vectors within the plane P).

In particular, if $\mathcal{A}$ is in general position (in the sense that every subset of n elements in $\mathcal{A}$ are affinely independent, or equivalently, every minimal reaction among the phases involves at least $n+1$ phases), the number of potential solutions is (cf. [17]*)*

$$2\left(1+\binom{n}{2}\right).$$

Proof. Since $\mathcal{A}^*$ lives in $\mathbb{R}^3$, there are four kinds of elements x in the lattice of flats:

- $x = \hat{0}$, having $\mu(\hat{0},\hat{0}) = +1$,
- $x = \ell$, a line spanned by a Gale vector a_i^*, having $\mu(\hat{0},\ell) = -1$,
- $x = P$, a 2-dimensional plane spanned by Gale vectors, having

$$\mu(\hat{0},P) = -\left(\mu(\hat{0},\hat{0}) + \sum_{\ell\subset P}\mu(\hat{0},\ell)\right) = m_P - 1, \textit{and}$$

- $x = \mathbb{R}^3$, having

$$\begin{aligned}\mu(\hat{0},\mathbb{R}^3) &= -\left(\mu(\hat{0},\hat{0}) + \sum_{\ell}\mu(\hat{0},\ell) + \sum_{P}\mu(\hat{0},P)\right)\\ &= -1 + \#\{\text{ lines } \ell \text{ spanned by Gale vectors}\}\\ &\quad + \sum_{P}(m_P - 1)\end{aligned}$$

Adding the absolute values of all of these gives the result stated in the Proposition.

In the generic case, since $\mathcal{A}$ has n points, there will be n distinct Gale vectors $\mathcal{A}^*$, no two of which span the same line ℓ, and there will be $\binom{n}{2}$ different planes P spanned by them ($\mathcal{A}$ is generic if and only if $\mathcal{A}^*$ is generic by matroid duality). Also, each of these planes will contain exactly two lines ℓ so $m_P - 1 = 1$. The second assertion follows from plugging these values into the first equation. □

Example 10.5. In Figure 12, the Euler sphere shown has 20 regions total (10 visible on the hemisphere shown, 10 more on the "underside"). One can compare this with the formula predicted in the proposition, which can be evaluated with the aid of the closed net picture of Gale vectors in Figure 11. This figure shows (the intersection with the sphere of) 8 planes P spanned by pairs of Gale vectors, namely

$$BC, BG, BW, DG, DC, DW, BD, BGW,$$

of which the first 7 have $m_P = 2$ and the last has $m_P = 3$. Thus the proposition would predict

$$2(1 + 7 \cdot (2 - 1) + 1 \cdot (3 - 1)) = 20$$

regions, as expected.

References

[1] M. Azaola and F. Santos, The graph of triangulations of a point configuration with $d + 4$ vertices is 3-connected. *Discrete Comput. Geom.* **23** (2000), 489–536.

[2] A. Björner, M. Las Vergnas, B. Sturmfels, N. White, and G. Ziegler, *Oriented Matroids*. Cambridge. Cambridge University Press, 1993.

[3] L.J. Billera, P. Filliman, and B. Sturmfels, Constructions and complexity of secondary polytopes. *Adv. Math.* **83** (1990), 155–179.

[4] L.J. Billera, I. M. Gelfand, and B. Sturmfels, Duality and minors of secondary polyhedra. *J. Combin. Theory Ser. B* **57** (1993), 258–268.

[5] R.G. Bland, and M. Las Vergnas, Orientability of matroids, *J. Combinatorial Theory* **B 24** (1978), 94–123.

[6] H. W. Day, Geometric analysis of phase equilibria in ternary systems of six phases. *Amer. J. Sci.* **272** (1972), 711–734.

[7] J.A. de Loera, S. Hoşten, F. Santos, B. Sturmfels, The polytope of all triangulations of a point configuration. *Doc. Math.* **1** (1996), No. 04, 103–119.

[8] J. Folkman and J. Lawrence, Oriented matroids. *J. Combinatorial Theory* **B 25** (1978), 199–236.

[9] D. Gale, Neighboring vertices on a convex polyhedron, in "Linear inequalities and related systems" (H.W. Kuhn and A.W. Tucker, eds.), *Annals of Math. Studies* **38**, Princeton Univ. Press, Princeton, 1956, pp. 255–263.

[10] I.M. Gelfand, M.M. Kapranov, A.V. Zelevinsky, *Discriminants, resultants, and multidimensional determinants*, Birkhäuser, Boston, MA, 1994.

[11] B. Grünbaum, *Convex Polytopes*, New York, Wiley Interscience, 1967.

[12] B. Guy and J. M. Pla, Structure of phase diagrams for n-component (n+k)-phase chemical systems: the concept of affigraphy, *Comptes Rendus de l'Academie des Sciences* **324 IIa** (1997), 1–7.

[13] T.J.B. Holland and R. Powell, R. An enlarged and updated internally consistent thermodynamic data set with uncertainties and correlations in the system $K_2O - Na_20 - CaO - MgO - MnO - FeO - Fe_2O_3 - Al_2O_3 - TiO_2 - SiO_2 - C - H_2 - O_2$ *Journal of Metamorphic Geology* **8** (1990), 89–124.

[14] C. L. Lawson, Transforming triangulations, *Discrete Math.* **3** (1972), 365–372.

[15] C.W. Lee, Regular triangulations of convex polytopes. *Applied geometry and discrete mathematics*, 443–456, *DIMACS Ser. Discrete Math. Theoret. Comput. Sci.* **4**, Amer. Math. Soc., Providence, RI, 1991.

[16] G. Kletetschka and J.H. Stout, Stability analysis of invariant points using Euler spheres, with an application to FMAS granulites. *J. metamorphic Geol.* **17** (1999), 1–14.

[17] R.E. Mohr and J.H. Stout, Multisystem nets for systems of $n + 3$ phases, *American Journal of Science* **280** (1980), 143–172.

[18] S.W. Peterson, CHEMOGALE: A Java applet for computing geochemical phase diagrams, 2000.
(Available at `www.math.umn.edu/~reiner/CHEMOGALE.html`)

[19] S.W. Peterson, *Oriented matroid analysis of thermochemical reaction systems*. Masters Thesis (2000), University of Minnesota, Minneapolis.

[20] J. Rambau, TOPCOM: Triangulations of Point Configurations and Oriented Matroids, version 0.2.0.
(Available at `www.zib.de/rambau/TOPCOM.html`.)

[21] J.E. Ricci, *The phase rule and heterogeneous equilibrium*, D. Van Nostrand Company, Inc., 1951.

[22] F. Santos, A point set whose space of triangulations is disconnected. *J. Amer. Math. Soc.* **13** (2000), 611–637.

[23] F. Santos, Non-connected toric Hilbert schemes, available at `http://arXiv.org/abs/math.CO/0204044`.

[24] F. Santos, Triangulations of oriented matroids. *Mem. Amer. Math. Soc.* **156** (2002), no. 741.

[25] F.A.H. Schreinemakers, In-, mono-, and di-variant equilibria, *Koninklijke Academia van Wetenschappen te Amsterdam* **18-28**(1915-1925), 322 p.

[26] A. Schrijver, *Theory of Linear and Integer Programming*, 1998, Wiley-Interscience, New York.

[27] V. S. Sheplev, Construction of chemographic diagrams. *Petrology* **4 1** (1996), 97–102.

[28] S.I. Usdansky, Some topological and combinatorial properties of c component $(c+4)$ phase multisystem nets. *Mathematical Geology* **19 8** (1987), 793–805.

[29] E. Zen, Some topological relationships in multisystems of $n+3$ phases I. General theory; unary and binary systems. *American Journal of Science* **264** (1966), 401-427.

[30] E. Zen Construction of pressure-temperature diagrams for multicomponent systems as the method of Schreinemakers- A geometric approach, *U.S. Geological Survey Bulletin 1225* (1966), 66 pp.

[31] E. Zen Some topological relationships in multisystems of $n+3$ phases II. Unary and binary metastable sequences. *American Journal of Science* **265** (1967), 871-897.

[32] E. Zen and E.H. Rosenboom Jr., Some topological relationships in multisystems of $n+3$ phases III. Ternary systems. *American Journal of Science* **272** (1972), 677-710.

[33] G.M. Ziegler,*Lectures on Polytopes*, New York, Springer-Verlag, 1995.

Dept. of Mathematics, Vanderbilt University, Nashville, TN 37240-0001
E-mail address: edelman@math.vanderbilt.edu

School of Mathematics, University of Minnesota, Minneapolis MN 55455
E-mail address: peterson@math.umn.edu

School of Mathematics, University of Minnesota, Minneapolis, MN 55455
E-mail address: reiner@math.umn.edu

Department of Geology and Geophysics, University of Minnesota, Minneapolis MN 55455
E-mail address: jstout@umn.edu